SMAR 2015 – Third Conference on Smart Monitoring,
Assessment and Rehabilitation of Civil Structures

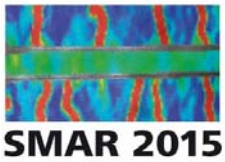

Strengthening of RC beams with iron-based shape memory alloy strips

Moslem Shahverdi, Christoph Czaderski, and Masoud Motavalli

Empa, Structural Engineering Research Laboratory, Dübendorf, Switzerland

ABSTRACT: Low cost Fe-Mn-Si based shape memory alloys (SMAs) can be a cost-effective alternative to the expensive Ni-Ti based shape memory alloys. The application of iron-based shape memory alloy (Fe-SMA) strips for structural strengthening of reinforced concrete (RC) beams is shown in this paper. The shape memory effect of the Fe-SMAs was used to prestress the concrete beams. The near surface mounted (NSM) strengthening technique was used in this study. The procedure for such application is as follows: first, the Fe-SMA strip has to be prestrained then it should be mounted into the grooves in the concrete cover. Afterwards the temperature in the Fe-SMA strip should be increased by resistive heating to provoke a phase transformation in the SMA. The full prestress develops when the material returns to environmental temperature. In the current study, three beams prestressed by Fe-SMA strips were compared with one beam strengthened by non-activated Fe-SMA strips, one beam strengthened by CFRP, and one beam un-strengthened. The higher cracking load and the smaller deflections proved that strengthening of RC beams with prestressed Fe-SMA strips worked well.

KEYWORDS: iron based shape memory alloy (Fe-SMA), prestress, activation, strengthening.

1 INTRODUCTION

Several existing concrete bridges have to be retrofitted due to aging or adapting for increasing the load capacity. A popular strengthening technique is the application of fiber reinforced polymer (FRP) strips or fabrics by means of epoxy adhesives on the concrete surface (Meier 1995). Beside this technique, another technique exists where the FRPs are inserted and glued in grooves in the concrete cover, what is termed as near surface mounted (NSM) strengthening (De Lorenzis et al. 2007). This strengthening method requires no surface preparation work but requires cutting the grooves. NSM strengthening provides better bonding, better protection against vandalism and fire and better durability compared to the externally bonded reinforcing technique.

In some cases, prestressed FRPs are applied for strengthening also. The advantages of prestressing are: the existing deformations and crack width can be reduced, the cracking and yielding loads will be higher, and the FRP material will be better utilized, (Motavalli et al. 2011). An overview of existing NSM prestressing systems used in laboratories is given in (El-Hacha et al. 2013).

Shape memory alloys (SMAs) have several unique properties. The most important properties are the shape memory effect and the superelasticity, (Janke et al. 2005). Due to the presence of the superelasticity property, SMAs are used in civil engineering applications as a passive

vibration damping and energy dissipation, (Janke, Czaderski et al. 2005). Iron based shape memory alloys were discovered by (Sato et al. 1982) in 1982. At Empa, an iron-based shape memory alloy (Fe–17Mn–5Si–10Cr–4Ni–1(V,C) (ma.-%)) has been developed in 2009, (Dong et al. 2009). Extensive explanation about these materials including some key properties such as the recovery stresses and the corrosion resistances of the materials are presented in (Cladera et al. 2014). In Japan, fishplates made of Fe-SMA have been used for prestressing of crane rail joints using (Maruyama et al. 2008, Maruyama et al. 2011) and for pipe joining (Maruyama and Kubo 2011).

Several investigations on prestressing of small concrete or mortar prisms by using shape memory alloys (SMAs) can be found in the literature, for example (Maji et al. 1998), (Czaderski et al. 2006), (Sawaguchi et al. 2006), (Sherif et al. 2014). Additionally, shape memory alloys are used for actively confine concrete cylinders, (Shin et al. 2010), large-scale concrete columns, (Shin et al. 2011) and non-circular concrete elements, (Chen et al. 2014). The advantages of such a prestressing technique compared to conventional prestressing is that there are no frictional losses due to the development of uniform tension force along the total length of a SMA tendon. In comparison to the conventional prestressing techniques, SMA tendons can be used for prestressing extremely thin concrete members without any need of anchors, oil hydraulic cylinders, ducts and grout injection. Preliminary experiments to investigate if the iron based shape memory alloys developed at Empa can be used as prestressed NSM were presented in the study (Czaderski et al. 2014), see also (Czaderski et al. 2015). In the current paper, experimental investigations on reinforced concrete (RC) beams strengthened with Fe-SMA strips are presented. For more details refer to (Shahverdi et al. 2015).

2 EXPERIMENTS

The experimental program was designed to demonstrate the feasibility of prestressed Fe-SMA strips for flexural strengthening of concrete beams. Experimental work was carried out at the Swiss Federal Laboratories for Materials Science and Technology (Empa) on six beams. Beams were constructed with the dimensions shown in Figure 1. All the beams were loaded in a four-point bending test scheme with a span of 2.0 m. One beam was used as the reference beam, four beams were strengthened by Fe-SMA strips, and one remaining beam was strengthened using one CFRP strip. A short description of each beam appears in Table 1.

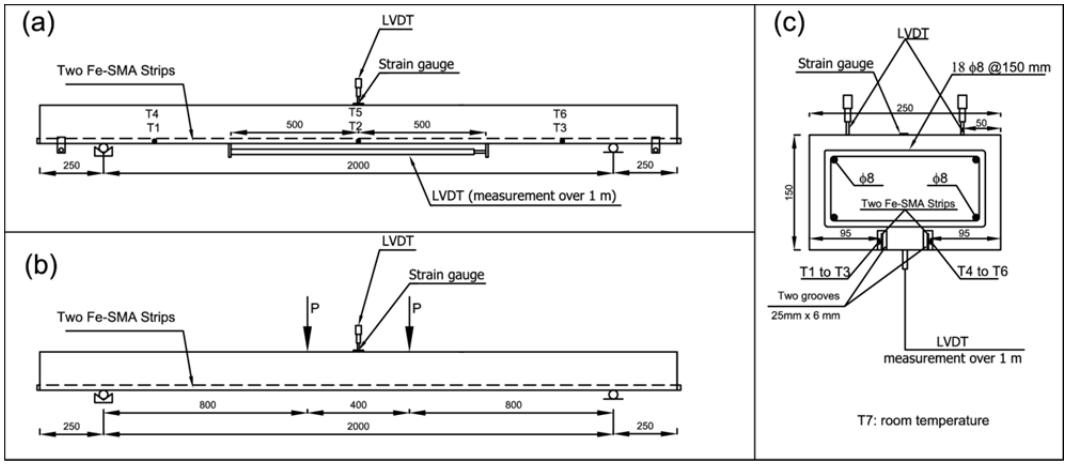

Figure 1: Drawing of Fe-SMA strengthened beams; a) setup for activation, b) setup for loading, and c) cross section of beams. T1 to T7 are thermocouple, all dimensions are in mm.

2.1 Materials

A concrete mix of Type I Portland cement and a coarse aggregate with a maximum size of 16 mm and water cement ratio of 0.50 by weight was used to cast the beams. Additional concrete samples of 150×150×150 mm were casted for each beam and were tested at the age of 28 days and at the day of performing the experiments. The average compressive strength, flexural tensile strength, and elastic modulus of the concrete after 28 days were respectively 53.4 MPa, 3.4 MPa, and 35.4 GPa. The CFRP strip (S&P Laminates CFK 150/2000) was received from S&P Clever Reinforcement in Seewen, Switzerland. The measured elastic modulus of the CFRP strip was around 150 GPa. The CFRP strips were glued into the grooves with an epoxy adhesive. However, the Fe-SMA strips were glued into the grooves with a cement-based mortar. Because the Fe-SMA strips should be activated by heating up to approximately 160 C in a short time, it would create problems in an epoxy adhesive having a glass transition temperature well below 160°C. The cement-based mortar was a flowable and expanding grout (SikaGrout-311) from Sika in Switzerland, and it was purchased from the market. According to the technical datasheet from the company, the maximum grain diameter size, compression strength after 28 days and elastic modulus of this mortar are 1.2 mm, 80–90 MPa and approximately 37.2 GPa, respectively.
The Empa iron-based shape memory alloy was used as prestressed NSM strengthening of reinforced concrete beams. This alloy was produced and manufactured in the form of strips in collaboration with two institutes in Austria and Germany and a German company as described in (Czaderski, Shahverdi et al. 2014). In order to ensure a good bond between the Fe-SMA strips and the concrete, ribs were applied on the strips by cold deforming (Figure 2). The ribs were applied at an angle of approximately 40° on one side and 130° on the other side of the strip to ensure a regular strain pattern along the strip, (Czaderski, Shahverdi et al. 2014).
The nominal thickness, initial width and the initial lengths were 1.7 mm, around 25 mm and more than 3 m respectively. However, these Fe-SMA strips were cut to 2.6 m long strips. The remaining short pieces of the strips were used for material characterization. Strips were grinded by a smooth sand paper on the edges, to remove edge cracks, and the final width of the strips was 20 mm.

2.2 Measurement set-up

The main experiments on the beams were performed in two phases: Phase 1, the activation of the 2.6 m long Fe-SMA strips embedded in grooves on the concrete cover and Phase 2, the four-point bending loading of the beams up to failure. Behavior of the examined beams were monitored and recorded during both phases by means of various monitoring devices including LVDTs, thermocouples, and strain gauges. The locations of these devices along the beams for the two phases are shown in Figure 1. Three type-K thermocouples with approximately 0.35 mm diameter were mounted on the surface of the SMA strips prior to embedding the Fe-SMAs in precut grooves. Deflections were measured using two LVDTs positioned at mid-span. The strains at the top and bottom sides of the mid-span were measured with a strain gauge and a LVDT, respectively.

2.3 Experimental procedure

The experimental procedure followed these main steps: a) prestraining of the Fe-SMA strips up to 2%, b) grouting of the Fe-SMA strips into the grooves, c) activation of Fe-SMA strips embedded in the concrete beams, and d) loading of the beams up to failure.

Table 1: Overview of examined beams with maximum obtained loads and corresponding deflections.

Beam No.	Strengthening with	P_{crack} (N)	P (N) at $\delta_{mid\text{-}span}$ =4mm	$\delta_{mid\text{-}span}$ (mm) at P=8 kN
1	reference beam, no strengthening	~1830	4039	17.00
2	strengthened by two SMA strips	~2470	6930	5.60
3	strengthened by two SMA strips and activated	~4490	7865	4.59
4	strengthened by two SMA strips and activated	~4740	8174	3.85
5	strengthened by one CFRP strip	~2390	5917	7.08
6	strengthened by two SMA strips and activated	~4180	7877	4.12

2.3.1 Prestraining and embedding the SMA strips

The Fe-SMA strips were prestrained to 2% elongation at room temperature, and then relaxed to a stress-free state with recovery of elastic strain. The SMAs were inserted into the grooves at the bottom of the beams which were made on a saw cut table machine in advance. The grooves were filled by a cement based grout prepared according to supplier recommendations (Figure 3). Finally, the excess grout was removed and the surface was leveled.

2.3.2 Activation of Fe-SMA strips

The activations were performed after the grout for the Fe-SMA strips was fully cured. The activations were done by resistive heating by means of a programmable electrical power supply (Figure 4). This power supply was controlled by a LabView program. The program acquired the signals from the thermocouples and controlled the current supply for resistive heating. When one of the thermocouples T1 to T3 or T4 to T6, measuring the strip temperature in the concrete, reached the target temperature of 160°C the power supply was switched off. Copper clamps (Figure 4) were used to secure contact between the cables from the power supply and the Fe-SMA strips.

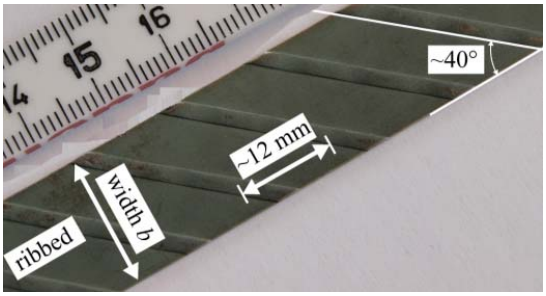

Figure 2: Detailed view of ribbed Fe-SMA strips.

Figure 3: Embedding Fe-SMA strips with cement based grout.

2.3.3 Beam loading

The beams were loaded using two 50 kN hydraulic actuators. The loading was under displacement control of one actuator at a rate of 0.02 mm/s. A side view of the experimental setup used in this study is shown in Figure 5. The beams were simply supported at the ends and were loaded using two concentrated loads with 400 mm spacing. Loading was applied in a quasi-static manner until a mid-span deflection of 4 mm equal to 1/500 of the beam span length was reached (serviceability limit state). After that, the beam was un-loaded until a mid-span deflection of 2 mm, then it was loaded again to the mid-span deflection of 4 mm. The loading-

unloading cycle was repeated five times for each beam. After the fifth loading cycle, the load was applied monotonically until the beam failure.

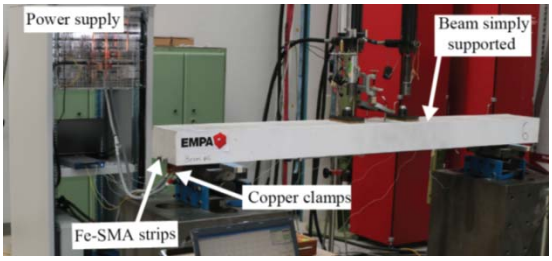

Figure 4: Beam No. 6 equipped for activation.

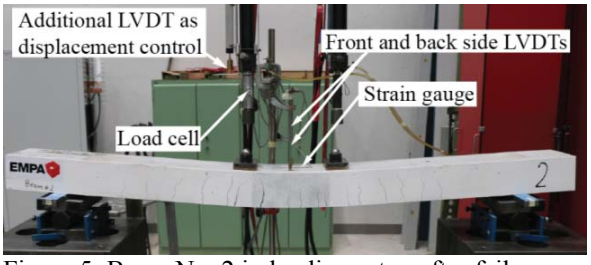

Figure 5: Beam No. 2 in loading setup after failure.

3 RESULTS AND DISCUSSIONS

3.1 Prestraining and recovery stresses

Stress–strain diagrams of prestrained specimens (long and short specimens) are given in Figure 6. Short strips were prestrained in a testing machine while long strips were prestrained by a manually operated oil-hydraulic jack. The unloading path after prestraining reached a strain of approximately 1.5%. Similar stress-strain curves of the two different experiments were observed.

A typical stress–temperature diagram of the short specimens with heating–cooling procedure for determination of the recovery stress is presented in Figure 7. The curve given in Figure 7 has a distinctive decrease of the stress until a temperature of approximately 40°C is reached. The decrease is attributed to the thermal expansion effect on the examined specimen. At temperatures higher than 40°C, the stress increases. This stress increase is attributed to phase transformation (from martensite to austenite), which causes the shape memory effect. The stress reaches in this case approximately 150 MPa at the temperature of 160°C. By cooling down the Fe-SMA strip, the stress increases further due to the thermal contraction effect. The inclination of the curve is approximately parallel to the starting part of the curve, which indicates similar coefficients of thermal expansion and elastic modulus for the two areas. At the end of the curve, the inclination of the curve decreases. This is attributed to a partial transformation from austenite to martensite. Finally, the obtained recovery stress at RT is reached.

3.2 Activation of the Fe-SMA strips embedded in beams

Mid-span deflection of the Beam No. 6 during and after activation is illustrated in Figure 8. It is visible, that the beam deformed at the beginning downwards due to temperature expansion, similar as in the characterization experiments presented in Figure 7. However, after a very short time, the activation of the Fe-SMA strips functioned and their prestressing reacted in the other direction and the beam deformed upwards. Figure 8 illustrates that a mid-span displacement of approximately 0.17 mm was reached after some hours when the beam was fully cooled down.

3.3 Loading behavior of beams

The load-mid-span deflection diagrams of all examined beams are depicted in Figure 9. In all examined beams, except Beam 5 (CFRP strengthened), three changes of the slope are evident. The first is due to concrete cracking, the second occurred when the internal steel reinforcement

began to yield and the third one occurred when the Fe-SMAs transformed in their low stiffness region, so called yielding of Fe-SMA. The load-deflection diagrams were linear prior to concrete cracking. After the concrete cracking the slope of the load-deflection decreased clearly. The cycling loading at the serviceability limit state did not have any clear effect on the slop and the load-deflection diagrams followed the same slope as prior to cycling loading.

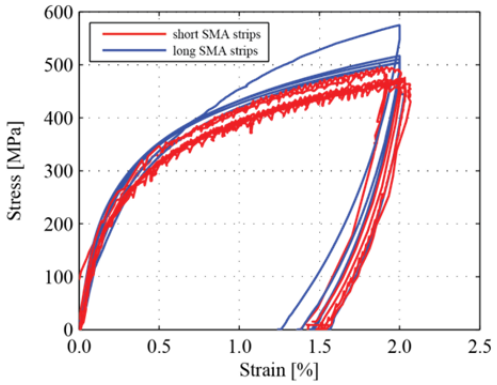

Figure 6: Prestraining of short and long strips.

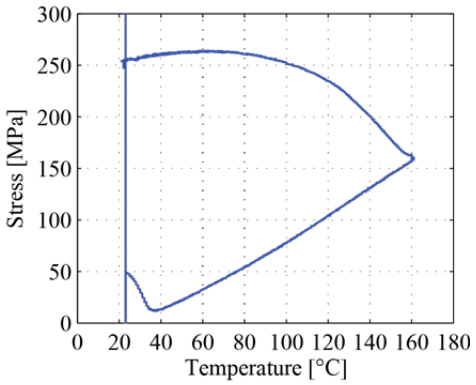

Figure 7: A typical recovery stress diagram of Fe-SMA strip specimen.

The failure of the reference beam, Beam No 1, occurred due to crushing of the concrete in compression after yielding of the longitudinal steel reinforcement. The maximum compressive strain measured by the strain gauge on the top of the beam at mid-span was 0.0035. The failure of the strengthened beam with one CFRP strip, Beam No 5, was associated with a sudden tensile failure of the CFRP strip, followed rapidly by concrete crushing at the top. In case of strengthened beams with Fe-SMA the failure was concrete crushing after yielding of longitudinal normal steel reinforcement and the so called yielding of Fe-SMA strips. However, maybe due to some edge micro-cracks in Fe-SMA strips, the failure modes of Beams No. 4 and 6 were concrete crushing after a tensile failure in one of the Fe-SMA strips.

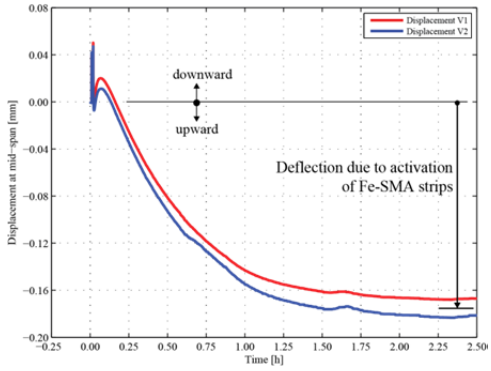

Figure 8: Behavior of Beam No. 6 during and after activation.

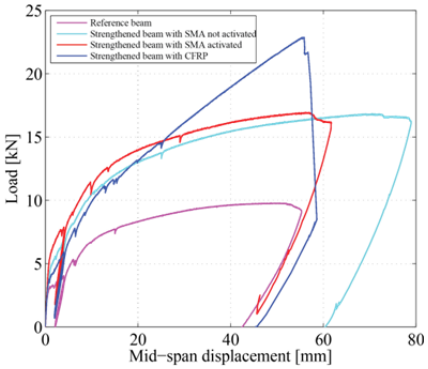

Figure 9: Load -mid-span displacement diagrams of the examined beams up to failure.

The corresponding loads for the first appearance of a concrete crack at the constant moment region of each examined beam (P_{crak}) are depicted in Table 1. The P_{crak} of strengthened beams were much higher than the reference one. Furthermore, by comparing the P_{crak} from Beam No. 2 with Beams No. 3, 4, and 6, the effect of prestressing is determined. The P_{crak} of the prestressed-Fe-SMA strengthened beams were up to 80% greater than the non-prestressed-Fe-SMA

strengthened beams. Comparison of the mid-span deflection of the examined beams at a load of 8 kN, shows that the reference beam exhibited the largest deflection; while, prestressed-Fe-SMA strengthened beams exhibited the smallest deflections. On the other hand, comparison of the obtained load capacity at a mid-span deflection of 4 mm (serviceability limit state), shows that the load capacity of the reference beam was the smallest and the load capacity of the prestressed-Fe-SMA strengthened beams was the highest. Beam No 5 with the CFRP strip (highest elastic modulus and strength, highest EA) had the highest failure load. However, Beam No 2 exhibited the largest deflection at failure as compared with the other strengthened beams. Obtained results show that the application of prestressed Fe-SMAs caused a decrease in beam deflection and consequently increase in load capacity at the serviceability limit state.

4 CONCLUSIONS

In the present study, the application of an iron-based shape memory alloy developed at Empa for RC beam strengthening is successfully demonstrated. In conclusion, the feasibility of ribbed Fe-SMA strips for strengthening and prestressing concrete beams has been shown. The following conclusions can be drawn:

1. Several innovative ideas have been successfully utilized including embedding of long Fe-SMA strips in grooves in the cover of concrete beams, activation of the Fe-SMA strips by a resistive heating approach, and application of Fe-SMAs as prestressed NSM strengthening.
2. The Fe-SMA strips were prestressed. This offers many advantages, including reduced crack widths, reduced deflections, reduced stress in the internal steel, and possibly increased fatigue resistance. Therefore, the serviceability and durability of structures can be improved.
3. The cracking load of the beams that were strengthened with prestressed Fe-SMA strips was on average 80% higher than the cracking load of a beam strengthened with the same Fe-SMA without prestressing.
4. Fe-SMA strips can more easily be prestressed than CFRP strips. Fe-SMAs can be prestressed even if they are embedded without need for a duct in the concrete because prestressing the SMAs does not require mechanical jacks and anchor heads.
5. The determined recovery stresses (i.e., prestresses after activation) were approximately 200 MPa.

Further study to demonstrate the application of Fe-SMA in real structures is pursuing in our group.

5 ACKNOWLEDGEMENT

This study was financially supported by the Swiss Commission for Technology and Innovation (CTI project 14496.1 PFIW-IW), which is greatly appreciated. Furthermore, thanks go to the Institute of Ferrous Metallurgy at the Montanuniversity Leoben in Austria, the Institute of Metal Forming at the TU Bergakademie Freiberg in Germany and the company G. Rau GmbH & Co. KG, Pforzheim in Germany, which produced the iron-based shape memory strips. Thanks go also to the company S&P Clever Reinforcement, Seewen, Switzerland, who provided the CFRP strip and the epoxy-based adhesive. Finally, the authors would like also to thank the company re-Fer AG in Wollerau, Switzerland, for their financial support.

6 REFERENCES

Chen, Q., M. Shin and B. Andrawes (2014). "Experimental study of non-circular concrete elements actively confined with shape memory alloy wires." *Construction and Building Materials* **61**: 303-311.

Cladera, A., B. Weber, C. Leinenbach, C. Czaderski, M. Shahverdi and M. Motavalli (2014). "Iron-based shape memory alloys for civil engineering structures: An overview." *Construction and Building Materials* **63**: 281-293.

Czaderski, C., B. Hahnebach and M. Motavalli (2006). "RC beam with variable stiffness and strength." *Construction and Building Materials* **20**(9): 824-833.

Czaderski, C., M. Shahverdi, R. Brönnimann, C. Leinenbach and M. Motavalli (2014). "Feasibility of iron-based shape memory alloy strips for prestressed strengthening of concrete structures." *Construction and Building Materials* **56**: 94-105.

Czaderski, C., B. Weber, M. Shahverdi, M. Motavalli, C. Leinenbach, W. Lee, R. Brönnimann and J. Michels (2015). Iron-based shape memory alloys (Fe-SMA) - a new material for prestressing concrete structures. SMAR 2015, Antalya, Turkey, 7-9 September 2015.

De Lorenzis, L. and J. G. Teng (2007). "Near-surface mounted FRP reinforcement: An emerging technique for strengthening structures." *Composites Part B-Engineering* **38**(2): 119-143.

Dong, Z., U. E. Klotz, C. Leinenbach, A. Bergamini, C. Czaderski and M. Motavalli (2009). "A novel Fe-Mn-Si shape memory alloy with improved shape recovery properties by VC precipitation." *Advanced Engineering Materials* **11**(1-2): 40-44.

El-Hacha, R. and K. Soudki (2013). "Prestressed near-surface mounted fibre reinforced polymer reinforcement for concrete structures - A review." *Canadian Journal of Civil Engineering* **40**(11): 1127-1139.

Janke, L., C. Czaderski, M. Motavalli and J. Ruth (2005). "Applications of shape memory alloys in civil engineering structures - Overview, limits and new ideas." *Materials and Structures* **38**(279): 578-592.

Maji, A. K. and I. Negret (1998). "Smart prestressing with shape-memory alloy." *Journal of Engineering Mechanics* **124**(10): 1121-1128.

Maruyama, T. and H. Kubo (2011). 12 - Ferrous (Fe-based) shape memory alloys (SMAs): properties, processing and applications. Shape Memory and Superelastic Alloys. K. Yamauchi, I. Ohkata, K. Tsuchiya and S. Miyazaki, Woodhead Publishing**:** 141-159.

Maruyama, T., T. Kurita, S. Kozaki, K. Andou, S. Farjami and H. Kubo (2008). "Innovation in producing crane rail fishplate using Fe-Mn-Si-Cr based shape memory alloy." *Materials Science and Technology* **24**(8): 908-912.

Meier, U. (1995). "Strengthening of structures using carbon fibre epoxy composites." *Construction and Building Materials* **9**(6): 341-351.

Motavalli, M., C. Czaderski and K. Pfyl-Lang (2011). "Prestressed CFRP for strengthening of reinforced concrete structures - recent developments at Empa Switzerland." *Journal of Composites for Construction, ASCE* **15**(2): 194-205.

Sato, A., E. Chishima, K. Soma and T. Mori (1982). "Shape memory effect in γ⇄ε transformation in Fe-30Mn-1Si alloy single crystals." *Acta Metallurgica* **30**(6): 1177-1183.

Sawaguchi, T., T. Kikuchi, K. Ogawa, S. Kajiwara, Y. Ikeo, M. Kojima and T. Ogawa (2006). "Development of prestressed concrete using Fe-Mn-Si-based shape memory alloys containing NbC." *Materials Transactions* **47**(3): 580-583.

Shahverdi, M., C. Czaderski and M. Motavalli (2015). " Iron-based shape memory alloys for prestressed near-surface mounted strengthening of reinforced concrete beams." *Construction & Building Materials*(submitted).

Sherif, M., O. Ozbulut, A. La and R. F. Hamilton (2014). Self-post-tensioning for concrete beams using shape memory alloys. ASME 2014 Conference on Smart Materials, Adaptive Structures and Intelligent Systems, SMASIS 2014.

Shin, M. and B. Andrawes (2010). "Experimental investigation of actively confined concrete using shape memory alloys." *Engineering Structures* **32**(3): 656-664.

Shin, M. and B. Andrawes (2011). "Lateral cyclic behavior of reinforced concrete columns retrofitted with shape memory spirals and FRP wraps." *Journal of Structural Engineering* **137**(11): 1282-1290.